

Effective reaction rates for diffusion-limited reaction cycles

Paweł Nałęcz-Jawecki and Paulina Szymańska

College of Inter-Faculty Individual Studies in Mathematics and Natural Sciences, University of Warsaw, Warsaw, Poland

Marek Kochańczyk

Institute of Fundamental Technological Research, Polish Academy of Sciences, Warsaw, Poland

Jacek Miękiś

Institute of Applied Mathematics and Mechanics, University of Warsaw, Warsaw, Poland

Tomasz Lipniacki*

*Institute of Fundamental Technological Research,
Polish Academy of Sciences, Warsaw, Poland and*

Department of Statistics, Rice University, Houston, Texas 77005, USA

Biological signals in cells are transmitted with the use of reaction cycles, such as the phosphorylation-dephosphorylation cycle, in which substrate is modified by antagonistic enzymes. An appreciable share of such reactions take place in crowded environments of two-dimensional structures, such as plasma membrane or intracellular membranes, and are expected to be diffusion-controlled. In this work, starting from the microscopic bimolecular reaction rate constants and using estimates of the mean first-passage time for an enzyme–substrate encounter, we derive diffusion-dependent effective macroscopic reaction rate coefficients (EMRRC) for a generic reaction cycle. Each EMRRC was found to be the half of the harmonic average of the microscopic rate constant (phosphorylation c or dephosphorylation d), and the effective (crowding-dependent) motility divided by a slowly decreasing logarithmic function of the sum of the enzyme concentrations. This implies that when c and d differ, the two EMRRCs scale differently with the motility, rendering the steady-state fraction of phosphorylated substrate molecules diffusion-dependent. Analytical predictions are verified using kinetic Monte Carlo simulations on the two-dimensional triangular lattice at the single-molecule resolution. It is demonstrated that the proposed formulas estimate the steady-state concentrations and effective reaction rates for different sets of microscopic reaction rates and concentrations of reactants, including a non-trivial example where with increasing diffusivity the fraction of phosphorylated substrate molecules changes from 10% to 90%.

This is an author-created manuscript of an article accepted for publication in the *Journal of Chemical Physics*, 2015, available via DOI: [10.1063/1.4936131](https://doi.org/10.1063/1.4936131). © 2015 AIP Publishing LLC.

I. INTRODUCTION

In numerous cellular information-processing pathways, signaling is initiated on the plasma membrane. Upon ligand binding, membrane receptors are modified chemically, which enables them to transfer the extracellular signal to the secondary, intracellular messengers. Due to the presence of membrane-anchored enzymes of antagonistic catalytic activity the activating modifications are reversible [1]. The membrane of mammalian cells of a diameter of order of 10 μm is considered to be a crowded environment, characterized by low diffusivity of order of 0.1–0.01 $\mu\text{m}^2/\text{s}$. Consequently, biochemical reactions on the plasma membrane are expected to be diffusion-controlled [2].

The aim of this study is to derive the diffusion-controlled *effective macroscopic reaction rate coefficients*, EMRRCs, in the cycle of antagonistic reactions. Such cycles, exemplified by the phosphorylation–dephosphorylation cycle, ubiquitination–deubiquitination cycle, acetylation–deacetylation cycle, or the GTPase cycle, allow for fast substrate reuse and are of fundamental importance in cellular signal transduction and amplification, enabling rapid transmission of extracellular signals to effector proteins such as transcription factors.

There have been numerous attempts to derive diffusion-dependent EMRRCs that govern processes in a macroscale chemical reactor. Most of the existing results, discussed in more detail in the Introduction to our previous study [3], involved relatively simple reaction schemes. In short, the irreversible reaction schemes included:

- $A + B \rightarrow C$ or $A + B \rightarrow \emptyset$ considered ini-

* Electronic mail: tlipnia@ippt.pan.pl

tially by von Smoluchowski [4] and later by, i.a., Collins and Kimball [5], Naqvi [6], Emais and Feher [7], Torney and McConnel [8], and Toussaint and Wilczek [9, 10];

- $A + B \rightarrow A + C$ and $A + B \rightarrow AB \rightarrow A + C$ studied by Szabo [11], Zhou [12], Kim et al. [13], and Park and Agmon [14, 15].

There were also many studies on reversible reaction schemes such as:

- $A + B \rightleftharpoons C$ considered by Zel'dovich and Ovchinnikov [16], Berg [17], Edelstein, Gopich, Agmon, and Szabo [18–21]. Takahashi et al. [22] studied a more complex, double phosphorylation–dephosphorylation cycle based on this simple reaction scheme, and Dushkek et al. [23] studied even longer chains of such cycles in membrane proteins. More recently, substrate rebinding was studied by van Zon et al. [24] and Govern et al. [25];
- $A + B \rightleftharpoons C + D$ studied by Agmon and colleagues [26–28], and by Szabo and Zhou [29].

In this theoretical work following our recent numerical study [3], we will investigate a phosphorylation–dephosphorylation cycle, which consists of two reactions: $K + S_u \rightarrow K + S_p$, $P + S_p \rightarrow P + S_u$. In this scheme, substrate molecules (S) assume either the phosphorylated (S_p) or unphosphorylated (S_u) state upon reactions with two antagonistic enzymes: kinase (K) and phosphatase (P). We will derive the EMRRCs and steady states as functions of the coefficient of diffusion and concentrations of the enzymes. The differences between single-reaction schemes and the cycle of two antagonistic reactions is caused by the fact that in the case of limited diffusion the antagonistic enzymes introduce heterogeneity in concentrations of phosphorylated and unphosphorylated substrate molecules. Because the EMRRCs depend both on diffusivity and microscopic reaction rate constants in the case when phosphorylation and dephosphorylation rate constants are different, the steady-state phosphorylated substrate fraction depends on diffusion. This is in contrast to a single-reaction scheme, such as reversible dimerization, in which the steady-state fraction of dimerized enzymes does not depend on diffusion (see, e.g., Ref. 21).

We will approach the microscopic limit by analyzing on-lattice Monte Carlo kinetics of diffusing molecules undergoing coupled reactions. In the previous study [3], we assumed that each lattice site can be either empty or occupied by a single molecule, and that phosphorylation and dephosphorylation reactions occur when substrate and enzyme molecules occupy adjacent lattice sites. Here, in contrast, we assume that substrate and enzyme molecules may enter the same lattice sites, and are required to be in the same lattice site in order to react. By the assumption that the substrate and enzyme molecules react only when present in the same lattice site, the reactions cease in the zero-diffusion limit. In the previous model, the substrate molecules having both

a kinase molecule and a phosphatase molecule at adjacent sites were repeatedly converted between the phosphorylated and the unphosphorylated states, which resulted in (sometimes significant) zero-diffusion contribution to the macroscopic reaction rates coefficients. In the present model there are no reactions firing in the zero-diffusion limit.

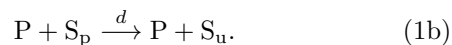
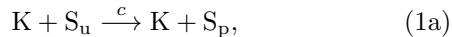
The paper is organized as follows: In the next section we introduce the model and numerical methods, and discuss simulations performed to verify theoretical predictions. The subsequent Results section is divided into four subsections in which we: 1) express the steady-state EMRRCs via the *mean first-passage time*, MFPT, in which a substrate molecule after changing its state upon the reaction with a given enzyme reaches an antagonistic enzyme molecule; 2) estimate this MFPT by the average number of steps, $w(\rho)$, until trapping a random walker in the system of randomly distributed traps with a given concentration, ρ ; 3) give final estimates for the steady-state EMRRCs and compare them with numerical results; 4) compare these results with those of our previous study [3]. Finally, in Conclusions we summarize and discuss the obtained results. The paper is supplemented by three appendices: In Appendix A we give estimates of effective motility which due to crowding is a function of the concentration of diffusing molecules. In Appendix B, the average number of steps until trapping, $w(\rho)$, is estimated numerically. In Appendix C we consider the reversible dimerization problem $A + B \rightleftharpoons C$ to show that for this classic example our on-lattice numerical simulations and theory agree with the steady-state analytical solution obtained in the Brownian dynamics scheme.

II. METHODS

A. Model

We consider a generic phosphorylation–dephosphorylation cycle in which two enzymes act antagonistically on the substrate, S, which upon interaction with the kinase, K, or the phosphatase, P, may assume either the phosphorylated state, S_p , or unphosphorylated state, S_u , respectively. The interacting molecules are confined to the two-dimensional membrane represented by the triangular lattice (in which each site has six neighbors) with periodic boundary conditions. Diffusion of molecules is modeled with stochastic hops to adjacent lattice sites. Possible events, which are diffusive hops and enzymatic reactions (phosphorylations and dephosphorylations), occur with propensities defined by motility, m , and microscopic reaction rate constants, c and d , respectively. The propensity of hopping to a neighboring allowed lattice site is $m/6$. We assume that neither two enzyme nor two substrate molecules can enter the same lattice site. The enzyme and the substrate molecules, however, may enter the same lattice site and have to be in the same lattice site to react

according to the following reaction scheme:



The molecules remain in the same lattice site after reacting, and then can leave the site independently with propensities defined by their motility. Microscopic phosphorylation and dephosphorylation rate constants, c and d , motility, m , and concentrations of the substrate, ρ_S , kinase, ρ_K and phosphatase, ρ_P , as well as the volume of the reactor (i.e., the total number of lattice sites), V , define the model. Concentrations ρ are defined as numbers of molecules per reactor volume, i.e., fractions of lattice sites occupied by molecules of a given type. Concentrations of phosphorylated and unphosphorylated substrate are denoted by ρ_{S_p} and ρ_{S_u} .

In the proposed approach the enzymatic reactions are modeled without considering explicitly the enzyme–substrate complex formation which allowed us to obtain analytical results. This assumption can be questionable in the case of high enzyme sequestration, however, in the case of the weak and moderate sequestrations the explicit inclusion of the enzyme–substrate complexation does not qualitatively influence the phosphorylated substrate fraction in equilibrium, as we demonstrated in our previous numerical study [3].

Our aim is to analytically derive formulas for the effective macroscopic reaction rate coefficients (EMRRCs), c_{eff} and d_{eff} , as functions of microscopic reaction rates c and d and the remaining parameters of the model. The EMRRCs are defined as:

$$c_{\text{eff}} = \frac{n_p}{\rho_{S_u} \rho_K V \Delta t}, \quad (2a)$$

$$d_{\text{eff}} = \frac{n_u}{\rho_{S_p} \rho_P V \Delta t}, \quad (2b)$$

where n_p and n_u are the numbers of phosphorylation and dephosphorylation reactions, respectively, that fired during a short time interval, Δt . We restrict our study to the steady-state values of EMRRCs, which can be determined by averaging over long time intervals.

When the number of molecules present in the system is large, EMRRCs govern the system of ordinary differential equations for ρ_{S_u} and ρ_{S_p} :

$$\frac{d}{dt} \rho_{S_u} = -c_{\text{eff}} \rho_K \rho_{S_u} + d_{\text{eff}} \rho_P \rho_{S_p}, \quad (3a)$$

$$\frac{d}{dt} \rho_{S_p} = c_{\text{eff}} \rho_K \rho_{S_u} - d_{\text{eff}} \rho_P \rho_{S_p}. \quad (3b)$$

These two equations are complementary, since their solutions satisfy $\rho_{S_u}(t) + \rho_{S_p}(t) = \rho_S = \text{const}$. The steady-state solution of Eqs. (3) is:

$$\rho_{S_u} = \frac{d_{\text{eff}} \rho_P}{c_{\text{eff}} \rho_K + d_{\text{eff}} \rho_P} \rho_S, \quad (4a)$$

$$\rho_{S_p} = \frac{c_{\text{eff}} \rho_K}{c_{\text{eff}} \rho_K + d_{\text{eff}} \rho_P} \rho_S. \quad (4b)$$

B. Numerical simulations

To verify the accuracy of the analytically derived formulas, the model will be analyzed by means of spatial kinetic Monte Carlo (KMC) simulations employing the software we described and used previously [3, 30, 31]. Before each step of the KMC simulation, a list of all possible events on the lattice is available. Time-step is drawn at random from the exponential distribution with the propensity parameter equal to the sum of the propensities of all possible events. A displacement or reaction event is selected from the complete list of events at random, with probability proportional to its propensity, and is executed. Then, before the next step, the list of all possible events is updated. Since the change in the system configuration after every simulation step is local, only a partial update of the list is necessary. By drawing events from the list which is always complete, there is no need to simulate trial events that would be subsequently rejected; this renders the method efficient. Such approach is equivalent to a stochastic simulation according to the Gillespie algorithm [32] applied to a spatially extended problem.

The EMRRCs were numerically estimated based on Eqs. (2) using long-run simulations performed on the 300×300 lattice (except for simulations shown in Fig. 1, which were performed on smaller lattices as indicated in the figure caption, and simulations for Fig. 2 (c), which were performed on the 1000×1000 lattice to estimate the dependence of accuracy of simulation-based estimates on the lattice size). For each analyzed set of parameters we performed 3 independent simulations which were long enough to allow for at least 3×10^4 reaction firings; only for simulations shown in Fig. 1 we performed 9 independent simulations, with at least 5×10^3 reactions each. This allowed us to determine the EMRRCs numerically with the relative error smaller than 1%.

We used the same simulation code to estimate the average number of steps made by a single random walker until trapping by one of randomly distributed immobile traps (see Appendix B). To analyze a broad range of trap concentrations, $\rho \in [0.0001; 0.1]$, simulations were performed on 1000×1000 lattices. The concentration of walkers was set to 0.001, which is a reasonable trade-off between the requirement of satisfactory statistics in a modest computational time and the requirement of a negligible number of collisions between walkers. After reaching a trap a walker was immediately degraded. Since traps are immobile, the computational cost is proportional to the number of remaining walkers, and thus the simulations speed up with time, which allowed us to perform simulations until all walkers were trapped. For each set of parameters, the simulations were performed 1000 times, so the calculation of the average number of steps before trapping was based on averaging over 10^6 walkers. Finally, the average number of steps was calculated as $w = m \times \tau_{\text{deg}}$, where τ_{deg} is the average time to walker degradation. To verify the accuracy of our method we performed analogous simulations in the case when an

analytical expression for w is known, i.e., when traps are distributed periodically [33].

The on-lattice numerical simulations have the obvious limitations resulting from space discretization. It is therefore important to verify whether the proposed approach leads to correct results, at least for the classic reverse dimerization problem, $A + B \rightleftharpoons A \cdot B \xrightleftharpoons[k]{q} C$, for which the analytical relation between the steady-state densities of A , B , and C molecules, $\rho_C = (k/q)\rho_A\rho_B$, is known for the Brownian-type dynamics. In Appendix C, we show that the same relation can be derived based on the on-lattice approach, in which dimers C arise from the geminate substrate pairs $A \cdot B$ that are formed when A and B molecules enter the same lattice site. We also demonstrate that this relation is satisfied by our numerical simulations to a good accuracy.

III. RESULTS

In the infinite-motility limit the probability of finding a given molecule is uniform on the lattice. Thus, at any time the concentration of enzyme–substrate pairs is given by the product of their concentrations: the kinase–unphosphorylated substrate pair concentration equals $\rho_K\rho_{S_u}$, and the phosphatase–phosphorylated substrate pair concentration equals $\rho_P\rho_{S_p}$. The numbers of phosphorylation and dephosphorylation reactions that fired during a time interval Δt in a reactor of volume V are $c\rho_K\rho_{S_u}V\Delta t$ and $d\rho_P\rho_{S_p}V\Delta t$, and thus from definitions in Eqs. (2) the EMRRCs in the infinite-motility limit are equal to:

$$c_{\text{eff}}^{\infty} = c, \quad d_{\text{eff}}^{\infty} = d. \quad (5)$$

In the case of finite motility, the concentration of enzyme–substrate pairs is smaller than the product of their concentrations so $c_{\text{eff}} < c$ and $d_{\text{eff}} < d$. This results from the spatiotemporal correlations: a substrate molecule located in the same lattice site as a kinase molecule has an increased chance of being in the phosphorylated state and, symmetrically, a substrate molecule located in the same lattice site as a phosphatase molecule has an increased chance of being in the unphosphorylated state.

A. Relation between MFPTs and EMRRCs

The steady-state fractions of unphosphorylated and phosphorylated substrate, ρ_{S_u}/ρ_S and ρ_{S_p}/ρ_S , can be expressed in terms of the average time intervals during which a substrate molecule remains unphosphorylated, τ_u , and phosphorylated, τ_p :

$$\frac{\rho_{S_u}}{\rho_S} = \frac{\tau_u}{\tau_u + \tau_p}, \quad \frac{\rho_{S_p}}{\rho_S} = \frac{\tau_p}{\tau_u + \tau_p}. \quad (6)$$

Now, using Eqs. (4) we can express c_{eff} and d_{eff} through τ_u and τ_p :

$$c_{\text{eff}} = \frac{1}{\tau_u\rho_K}, \quad d_{\text{eff}} = \frac{1}{\tau_p\rho_P}. \quad (7)$$

To calculate time intervals τ_u and τ_p we split them into:

$$\tau_u = \tau_{u_1} + \tau_{u_2}, \quad \tau_p = \tau_{p_1} + \tau_{p_2}, \quad (8)$$

where τ_{u_1} (τ_{p_1}) is MFPT in which a substrate molecule after being modified by a phosphatase (kinase) molecule meets a kinase (phosphatase) molecule for a first time, and τ_{u_2} (τ_{p_2}) is the average time after which a substrate molecule occupying initially the same lattice site as a kinase (phosphatase) molecule becomes phosphorylated (unphosphorylated).

Time intervals τ_u and τ_p depend on the effective motilities of enzyme and substrate molecules, \tilde{m}_E and \tilde{m}_S . The effective motilities are lower than the nominal motility of all molecules, m , due to molecular crowding, and when $\rho_E \neq \rho_S$, then \tilde{m}_E and \tilde{m}_S differ because enzyme and substrate molecules are crowding agents only for themselves. The effective relative motility of enzyme and substrate molecules is $\tilde{M} = \tilde{m}_E + \tilde{m}_S$. The time between encounters of enzyme and substrate molecules scales inversely with \tilde{M} . Following the original paper by van Beijeren and Kutner [34] and our previous study [3], we provide approximate formulas for \tilde{m}_E and \tilde{m}_S in Appendix A.

We first calculate τ_{u_2} . When an unphosphorylated substrate molecule and a kinase molecule meet in the same lattice site, two exclusive events are possible: either the substrate molecule gets phosphorylated or the molecules move apart before the reaction fires. The expected time for which an unphosphorylated substrate molecule and a kinase molecule remain in the same lattice site, τ_{short} , is inversely proportional to the sum of rates of these two events, $\tau_{\text{short}} = 1/(c + \tilde{M})$. With the probability of the phosphorylation event, which is $c/(c + \tilde{M})$, τ_{u_2} will be equal to τ_{short} , and with the probability of the separation event, which is $\tilde{M}/(c + \tilde{M})$, τ_{u_2} will be equal to τ_{long} , which is the expected time for substrate molecule phosphorylation in the case when it moves away from the kinase molecule. Taken together, τ_{u_2} can be expressed as:

$$\tau_{u_2} = \frac{c}{c + \tilde{M}}\tau_{\text{short}} + \frac{\tilde{M}}{c + \tilde{M}}\tau_{\text{long}}, \quad (9)$$

where

$$\tau_{\text{long}} = \tau_{\text{find}} + \tau_{\text{short}} + \tau_{u_2}. \quad (10)$$

Here, τ_{find} is the average time for the substrate molecule to meet a kinase molecule (the same or another) under the condition that it is in a site adjacent to a site occupied by a kinase molecule. When the substrate molecule meets a kinase molecule, the initially considered situation reoccurs and therefore the third term is τ_{u_2} .

To calculate τ_{find} let us notice that since the fraction of lattice sites occupied by kinase molecules is equal to

ρ_K , on average every $1/\rho_K$ steps the substrate molecule meets a kinase molecule. This is, when a substrate molecule and a kinase molecule occupy the same lattice site, the expected number of steps after which the substrate molecule meets the same or another kinase molecule is $1/\rho_K$. Therefore, if these two molecules are located in adjacent lattice sites, i.e., when one step toward next meeting has already been done, the expected number of steps is $1/\rho_K - 1$. Thus

$$\tau_{\text{find}} = \frac{1/\rho_K - 1}{\tilde{M}}. \quad (11)$$

Finally, Eq. (9), Eq. (10), and Eq. (11) together yield

$$\tau_{u_2} = \frac{c}{c + \tilde{M}} \frac{1}{c + \tilde{M}} + \frac{\tilde{M}}{c + \tilde{M}} \left(\frac{1/\rho_K - 1}{\tilde{M}} + \frac{1}{c + \tilde{M}} + \tau_{u_2} \right), \quad (12)$$

from which we obtain a simple expression for τ_{u_2} and an analogous expression for τ_{p_2} :

$$\tau_{u_2} = \frac{1}{c\rho_K}, \quad \tau_{p_2} = \frac{1}{d\rho_P}. \quad (13)$$

To complete calculations of τ_u and τ_p we need to estimate τ_{u_1} and τ_{p_1} . These two MFPTs can be expressed as:

$$\tau_{u_1} = \frac{w(\rho_P, \rho_K)}{\tilde{M}}, \quad \tau_{p_1} = \frac{w(\rho_K, \rho_P)}{\tilde{M}}, \quad (14)$$

where $w(\rho_P, \rho_K)$ and $w(\rho_K, \rho_P)$ are the expected numbers of steps needed for a substrate molecule to reach a kinase and phosphatase molecule, respectively, after being converted by a phosphatase (kinase) molecule. Eventually, we arrive at the following formulas:

$$c_{\text{eff}} = \frac{1}{(\tau_{u_1} + \tau_{u_2})\rho_K} = \left(\frac{1}{c} + \frac{\rho_K w(\rho_P, \rho_K)}{\tilde{M}} \right)^{-1}, \quad (15a)$$

$$d_{\text{eff}} = \frac{1}{(\tau_{p_1} + \tau_{p_2})\rho_P} = \left(\frac{1}{d} + \frac{\rho_P w(\rho_K, \rho_P)}{\tilde{M}} \right)^{-1}. \quad (15b)$$

B. Estimation of MFPTs

The MFPTs τ_{u_1} and τ_{p_1} , Eqs. (14), are simple functions of $w(\rho_P, \rho_K)$ and $w(\rho_K, \rho_P)$ which need to be estimated.

Under the assumption that the search for enzyme molecules of an appropriate type starts from a random position, functions $w(\rho_P, \rho_K)$ and $w(\rho_K, \rho_P)$ can be simplified to

$$w(\rho_P, \rho_K) = w(\rho_K), \quad w(\rho_K, \rho_P) = w(\rho_P). \quad (16)$$

To understand when the above simplifying assumption is valid, let us consider the case when on the lattice there is only one kinase molecule and a large number of phos-

phatase molecules. In such a case, a substrate molecule phosphorylated on the kinase molecule will be dephosphorylated in its vicinity by one of numerous phosphatase molecules, and therefore the next search for the single kinase molecule will start not from a random position with respect to the kinase molecule but more likely from its vicinity. Thus, in the considered case, the assumption is not valid for the phosphorylation reaction; however, since there is only one kinase molecule and thus the expected time to phosphorylation is relatively long, the abundant phosphatase molecules change significantly their positions between two dephosphorylation reactions, so that one can assume that the search for a phosphatase molecule starts from a random position with respect to positions of phosphatase molecules.

Now, let us consider the system of N different enzyme molecules, E_i , $i = 1, \dots, N$, and assume that each enzyme molecule E_i converts substrate molecules to the distinct state S_i with reaction rate q . Let us assume that $N \gg 1$ and let ρ_E denote the total concentration of all enzyme molecules. In light of the observation made in the previous paragraph, substrate molecules converted by E_i (i.e., in state S_i) will start their search for the remaining $N - 1$ enzyme molecules at a position that can be considered random (with respect to remaining enzyme molecules). Thus, the average time τ for which the substrate molecules will remain in each of states S_i is (by analogy to Eqs. (8), with Eqs. (13) and Eqs. (14), and since the concentration of $N - 1$ enzyme molecules is $\approx \rho_E$)

$$\tau = \frac{1}{q\rho_E} + \frac{w(\rho_E)}{\tilde{M}}. \quad (17)$$

The number of reactions per substrate molecule, per time, is equal to $r = 1/\tau$. Let us assume that one part of these enzyme molecules are kinase molecules and the rest are phosphatase molecules, so that $\rho_K + \rho_P = \rho_E$. Therefore, the probability that an unphosphorylated substrate molecule will be converted in the next reaction to the phosphorylated state is ρ_K/ρ_E , while with the probability of ρ_P/ρ_E it will be converted to another unphosphorylated state (such pseudo-conversions are possible because we assumed that each enzyme molecule converts the substrate to a distinct state). The number of real phosphorylation reactions (i.e., conversions from the unphosphorylated to the phosphorylated state) per unphosphorylated substrate molecule is $r_p = r \times \rho_K/\rho_E$, and therefore the average time spent by a substrate molecule in the unphosphorylated state is $\tau_u = 1/r_p = \tau \times \rho_E/\rho_K$.

From $c_{\text{eff}} = 1/(\tau_u \rho_K)$, Eqs. (7), we obtain

$$c_{\text{eff}} = \left(\frac{1}{q} + \frac{1}{\tilde{M}} \rho_E w(\rho_E) \right)^{-1}. \quad (18)$$

To derive the above equation we had to assume that all substrate states, S_i , are equiprobable, which requires $c = d = q$. In the case when $c \neq d$ we propose to replace q by c or d , appropriately, which leads to the following

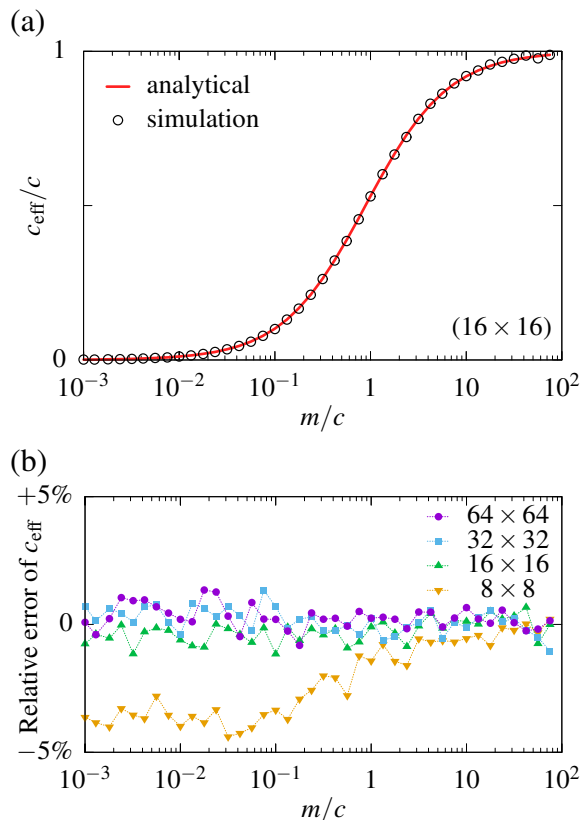


FIG. 1. Single enzyme pair model, analytical expression in Eqs. (21) versus numerical estimates. (a) Normalized effective phosphorylation rate coefficient c_{eff}/c as a function of m/c for a reactor of size 16×16 . (b) Relative percentage error of c_{eff} for four reactor volumes V : 8×8 , 16×16 , 32×32 , and 64×64 . For both panels $c = d$ and $\rho_K = \rho_P = 1/V$.

approximations for EMRRCs:

$$c_{\text{eff}} = \left[\frac{1}{c} + \frac{1}{\tilde{M}} (\rho_K + \rho_P) w(\rho_K + \rho_P) \right]^{-1}, \quad (19a)$$

$$d_{\text{eff}} = \left[\frac{1}{d} + \frac{1}{\tilde{M}} (\rho_K + \rho_P) w(\rho_K + \rho_P) \right]^{-1}, \quad (19b)$$

where, recall, $w(\rho)$ is the average number of steps until trapping a random walker in a system of randomly distributed traps of concentration ρ .

C. Final formulas and their numerical verification

As shown in Appendix B, $w(\rho) = w(1/V)$, where V is the volume of a reactor containing a single trap or a trap-specific volume in a reactor with traps of concentration ρ , can be approximated by the following asymptotic formula [33]:

$$w(1/V) = \alpha V \log V + \beta V + \mathcal{O}(1). \quad (20)$$

For the triangular lattice and a square-shaped reactor with periodic distribution of traps (or, equivalently, on finite lattices of volume $V = 1/\rho$ with periodic boundary conditions containing a single trap) coefficients were calculated by Montroll [33] and are as follows: $\alpha = \sqrt{3}/(2\pi)$, $\beta \approx 0.235$. When traps are distributed randomly, coefficients α' and β' were estimated numerically. After assuming $\alpha' = \alpha$ we obtained a good fit for $\beta' = 1.00$ (see Appendix B).

One can use Eq. (20) with coefficients α, β to estimate the effective reaction rate coefficients in idealized systems which in volume V contain a single pair of antagonistic enzyme molecules. In this case we return to Eqs. (15) and, because in this case the substrate molecule searches always for a single enzyme molecule (kinase or phosphatase), we set $w(\rho_K, \rho_P) = w(\rho_P, \rho_K) = w(1/V)$. In this way we obtain the following expressions for c_{eff} and d_{eff} :

$$c_{\text{eff}} = \left(\frac{1}{c} + \frac{\alpha \log V + \beta}{\tilde{M}} \right)^{-1}, \quad (21a)$$

$$d_{\text{eff}} = \left(\frac{1}{d} + \frac{\alpha \log V + \beta}{\tilde{M}} \right)^{-1}. \quad (21b)$$

In Fig. 1, we study the fully symmetric case ($c = d$) for a single pair of enzyme molecules and show that the formulas in Eqs. (21) agree satisfactorily with results of numerical simulations. In panel (a) we plot the dependence of c_{eff} on the speed of diffusion for an example reactor of size 16×16 . In panel (b) we show the relative error of our approximation for different sizes of the reactor, with always one kinase molecule, one phosphatase molecule, and one substrate molecule present in the reactor. We observe that for reactors of size 16×16 or larger the discrepancy between formulas in Eqs. (21) and results of numerical simulations is lower than 2%.

To obtain the EMRRCs in the limit of large reactor volume, with multiple enzyme molecules, we use our estimates of $w(\rho) = w(1/V)$ in the case when traps are randomly distributed (Appendix B). After setting $1/V = \rho_K + \rho_P$ from Eqs. (19) we obtain

$$c_{\text{eff}} = \left[\frac{1}{c} + \frac{1}{\tilde{M}} \left(\alpha' \log \frac{1}{\rho_K + \rho_P} + \beta' \right) \right]^{-1}, \quad (22a)$$

$$d_{\text{eff}} = \left[\frac{1}{d} + \frac{1}{\tilde{M}} \left(\alpha' \log \frac{1}{\rho_K + \rho_P} + \beta' \right) \right]^{-1}, \quad (22b)$$

with $\alpha' = \alpha = \sqrt{3}/(2\pi)$, $\beta' = 1.00$. The steady-state concentrations of phosphorylated and unphosphorylated substrate fractions are given by Eqs. (4).

In the next four figures we compare the EMRRCs given by Eqs. (22) with numerical estimates. First, in Fig. 2, we consider the fully symmetric case in which $c = d$ and $\rho_K = \rho_P$. For substrate density $\rho_S \leq 0.1$ and enzyme densities $\rho_K, \rho_P \leq 0.03$ the relative error of c_{eff} , (simula-

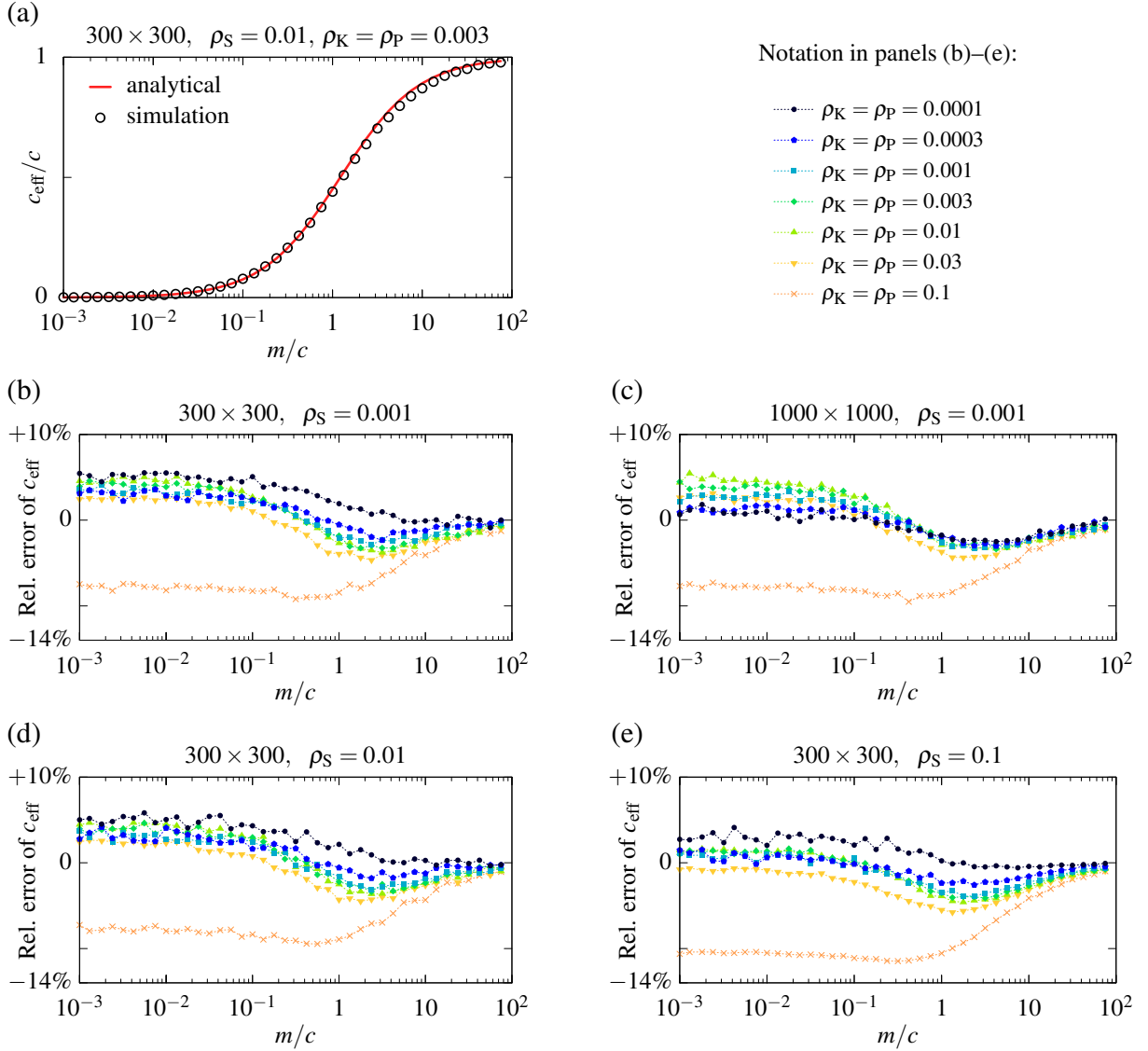


FIG. 2. Comparison of analytical expressions in Eqs. (22) with numerical estimates in the fully symmetric case of $c = d$, $\rho_K = \rho_P$. (a) Normalized effective phosphorylation rate coefficient c_{eff}/c for $\rho_K = \rho_P = 0.003$ and substrate concentration $\rho_S = 0.01$. (b)–(e) Relative error of c_{eff} , i.e., (simulation value – analytical value)/analytical value, for seven values of $\rho_K = \rho_P \in \{0.0001; 0.1\}$. The substrate concentrations are: $\rho_S = 0.001$ in panels (b) and (c), $\rho_S = 0.01$ in panel (d), and $\rho_S = 0.1$ in panel (e). Simulations for panel (c) were performed on the 1000×1000 lattice while remaining simulations were performed on 300×300 lattice. Please notice the difference between the relative errors of c_{eff} for the lowest enzyme densities (black dots) obtained in simulations performed on 300×300 and 1000×1000 lattices.

tion value – analytical value)/analytical value, remains below 5% and decreases with the enzyme density. This is visible in Fig. 2(c), for which simulations were performed on the 1000×1000 lattice. The remaining simulations were performed (for technical limitations) on the smaller 300×300 lattice, for which at the lowest enzyme concentration, $\rho_K = \rho_P = 10^{-4}$, the number of kinases (and phosphatases) is $N = 9$, and therefore the condition $N \gg 1$ is not satisfied. The comparison of the results obtained in the simulation performed on the 300×300 and 1000×1000 lattices suggests that at least part of the discrepancy between the theory and simulations is introduced by the small size of the lattice.

In Fig. 3 we consider the case in which $c = d$, but

$\rho_K \neq \rho_P$. Let us notice that Eqs. (22) together with Eqs. (4) imply that when $c = d$,

$$\frac{\rho_{S_p}}{\rho_S} = \frac{\rho_K}{\rho_K + \rho_P}. \quad (23)$$

Figure 3(a) shows a perfect agreement, with error less than 0.002, of Eq. (23) and the numerical estimate; Figure 3(b)–3(c) show that EMRRCs are predicted with the accuracy of about 5%.

In Fig. 4 we consider asymmetric cases in which $c = 10d$ (first column) or $c = 100d$ (second column). In the third column we show results for the fully asymmetric case in which $c = 100d$ and $\rho_K = 0.1\rho_P$. In this case,

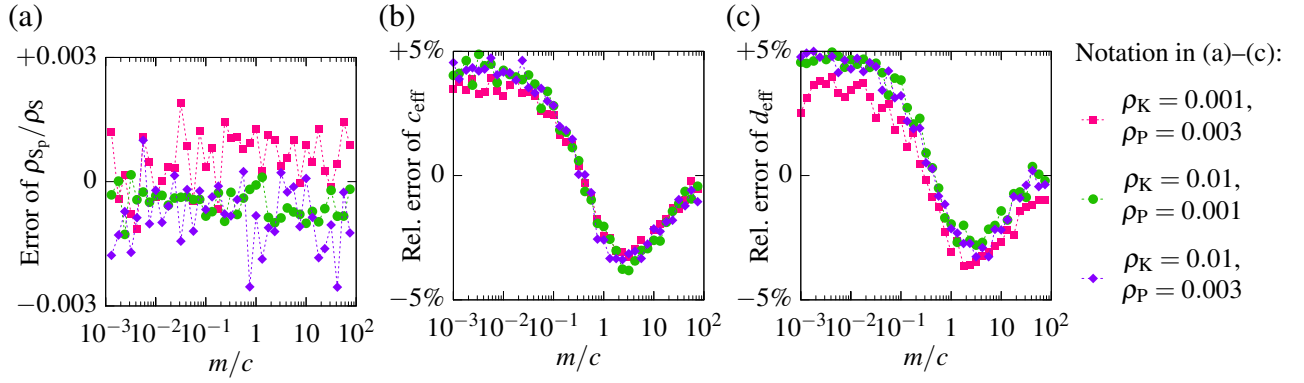


FIG. 3. Comparison of analytical expressions in Eqs. (22) and Eq. (23) versus numerical estimates. (a) Error of ρ_{S_p}/ρ_S . (b), (c) Relative error of c_{eff} and d_{eff} . Three pairs of ρ_K and ρ_P were assumed: $\rho_K = 0.001, \rho_P = 0.003$ (pink squares); $\rho_K = 0.01, \rho_P = 0.001$ (green circles); and $\rho_K = 0.01, \rho_P = 0.003$ (violet diamonds). In all panels the substrate concentration is $\rho_S = 0.01$ and $c = d$.

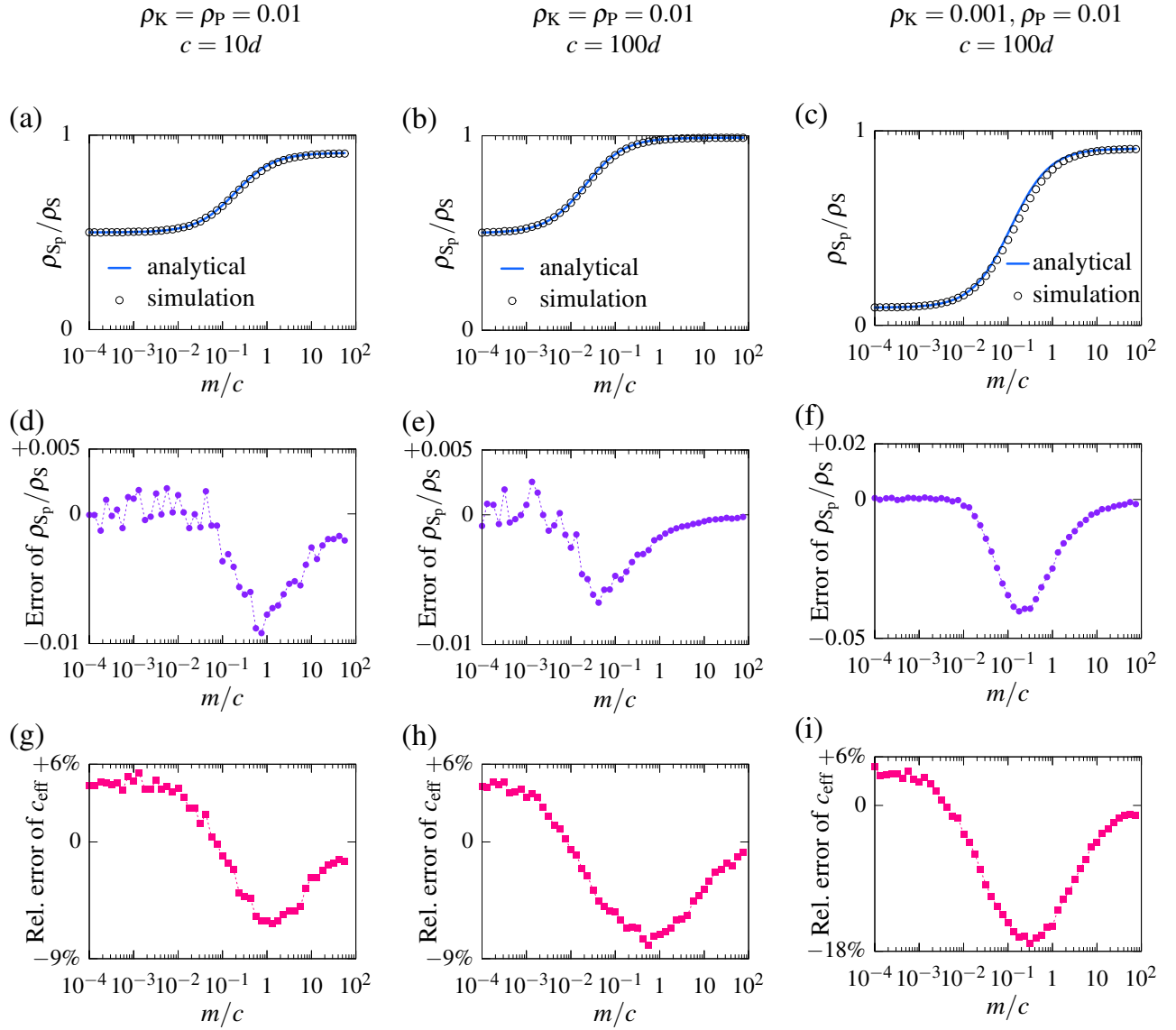


FIG. 4. Comparison of analytical expressions in Eqs. (22) and (4) versus numerical estimates. First row (panels (a)–(c)) shows phosphorylated substrate fraction ρ_{S_p}/ρ_S , second row (panels (d)–(f)) shows error of ρ_{S_p}/ρ_S , i.e., (simulation value – analytical value), third row (panels (g)–(i)) shows relative error of c_{eff} . In the first column (panels (a), (d), (g)) $c = 10d$ and in the second column (panels (b), (e), (h)) $c = 100d$; in the first and the second column $\rho_K = \rho_P = 0.01$. In the third column (panels (c), (f), (i)) $c = 100d$ with $\rho_K = 0.001, \rho_P = 0.01$. Substrate concentration is $\rho_S = 0.01$ for all panels.

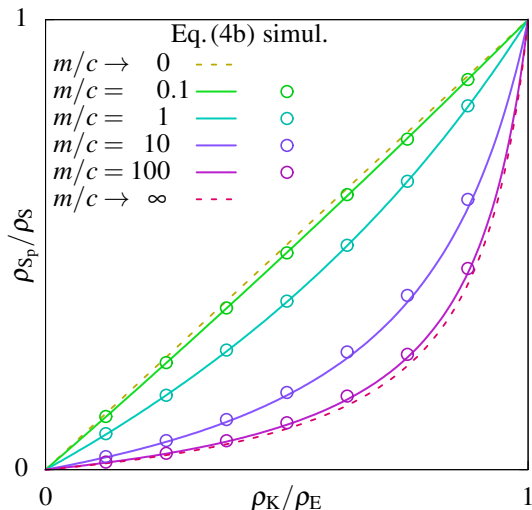


FIG. 5. Fraction of phosphorylated substrate ρ_{S_p}/ρ_S as a function of enzymes ratio ρ_K/ρ_E in the case when the phosphatase activity is 10 times higher than the kinase activity, $d = 10c$. Concentrations: $\rho_E = \rho_K + \rho_P = 0.006$ and $\rho_S = 0.01$.

in the limit of infinite diffusion, i.e., when $c_{\text{eff}} = c$ and $d_{\text{eff}} = d$, phosphorylation proceeds at the effective rate $\propto c \times \rho_K$ that is ten times greater than the effective dephosphorylation rate $\propto d \times \rho_P$. Consequently, the fraction of phosphorylated substrate is close to 0.9. In the opposite, diffusion-controlled limit, $c_{\text{eff}} \approx d_{\text{eff}}$ and therefore since phosphatase molecules are ten times more abundant, dephosphorylation proceeds ten times faster than phosphorylation, and as a result the phosphorylated substrate fraction is close to 0.1. This example demonstrates that the speed of diffusion can qualitatively influence the steady state of the system.

Finally, in Fig. 5 we consider the case when the phosphatase activity is 10 times higher than the kinase activity, $d = 10c$, and calculate the fraction of the phosphorylated substrate as a function of enzymes ratio. Four different motility values are considered. The results obtained for $m/c = 0.1$ lie close to those for the zero-diffusion limit, $m/c \rightarrow 0$, for which $\rho_{S_p}/\rho_S = \rho_K/(\rho_K + \rho_P)$; the results obtained for $m/c = 100$ lie close to those for the limit of infinite diffusion, $m/c \rightarrow \infty$, for which $\rho_{S_p}/\rho_S = c\rho_K/(c\rho_K + d\rho_P)$.

D. Comparison with the previous study

As mentioned in the Introduction, this study follows our previous numerical study [3] in which the same reaction scheme was considered under the assumption that each lattice site can be occupied by no more than one molecule, and that an enzyme molecule reacts with a substrate molecule when located in adjacent lattice sites. Here, in contrast, we assumed that enzyme and substrate molecules are allowed to enter the same lattice site, and have to be in the same lattice site in order to react. This assumption substantially simplifies the problem and al-

lowed us to obtain the (approximate) analytical results.

Let us compare predictions of these two models. The assumption in the former model [3] implies a larger interaction radius and causes that there are on average six times more enzyme–substrate pairs than in the current model, thus in the infinite-diffusion limit the EMRRC was equal $c_{\text{eff}}^\infty = 6c$ (not just c as in the current model). Therefore, to compare the two models (Fig. 6), in the simulations according to the former model we divide microscopic constants c and d by 6, and normalize c_{eff} with respect to c_{eff}^∞ for both models. The increase of the reaction radius caused that the effective distances between enzymes shortened, which for finite motility increased the EMRRCs with respect to the current model, Fig. 6 (a) and (b). Additionally, because of the larger reaction radius the substrate molecules could have two antagonistic enzymes in their reaction volumes (consisting of six neighboring sites). Substrates having (at least) two antagonistic neighbors were sequentially phosphorylated and dephosphorylated, which led to nonzero c_{eff} in the zero-motility limit. The zero-motility EMRRCs are significant when the probability of having two antagonistic enzymes is large, i.e. for dense systems, Fig. 6 (a). In reality, however, the sequential substrate modifications by the neighboring enzymes require the substrate molecule to expose its modified residue to the antagonistic enzyme. One can thus expect that in the case when both translational and rotational diffusion cease, the reactions are suppressed and therefore the EMRRCs should converge to zero in the limit of zero (translational and rotational) diffusion (as implicated by the current model).

Fig. 6 (c) shows the discrepancy between steady-state phosphorylated substrate fractions predicted by two models, which arises when $c \neq d$ (for $c = d$, both models predict that $\rho_{S_p}/\rho_S = \rho_K/(\rho_K + \rho_P)$ independently of motility).

We expect that in the parameter region in which the discrepancy between these two models is significant (i.e., for very small motility and high enzyme concentration), the discrete lattice-based approach breaks, and the analysis should be based on the rigid body Brownian dynamics. The simulations should account for refractory times of enzyme molecules, ATP exchange kinetics, and for orientation of substrate and enzyme molecules.

IV. CONCLUSIONS

We derived formulas for the diffusion-controlled effective macroscopic reaction rate coefficients in a cycle of two reactions in which two antagonistic enzymes (here: kinase and phosphatase) modify the state of a substrate. Such cycles are ubiquitously utilized in biochemical signal transduction because they allow for rapid information transmission: substrate molecules are reused instead of being degraded and resynthesized.

We focused on two-dimensional reactors, which have their own peculiarities and are substantially different from three-dimensional reactors, but play an important

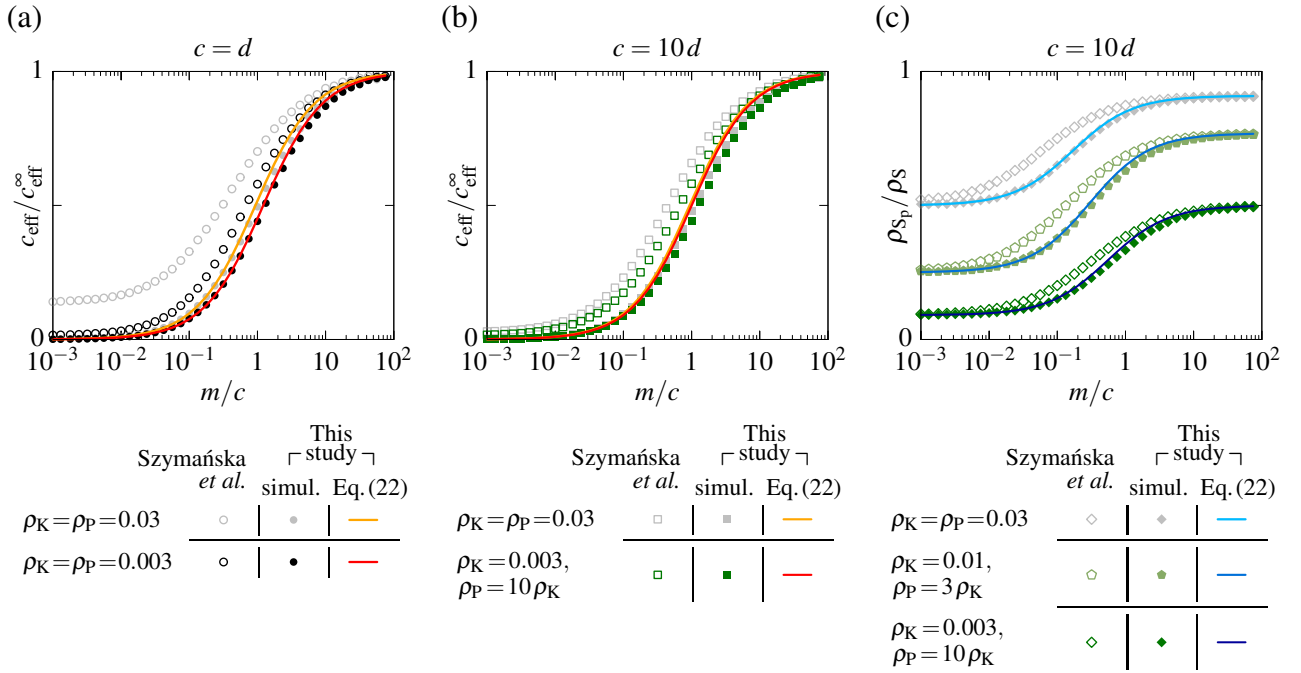


FIG. 6. Comparison of the current model with the model by Szymańska *et al.* [3]. Solid lines present theoretical predictions of the current model. (a) Normalized effective phosphorylation rate coefficient, $c_{\text{eff}}/c_{\text{eff}}^{\infty}$, in the fully symmetric case: $c = d$, $\rho_K = \rho_P$ with ρ_K equal 0.03 or 0.003. (b) Normalized effective phosphorylation rate coefficient, $c_{\text{eff}}/c_{\text{eff}}^{\infty}$, in the asymmetric case $c = 10d$, with $\rho_P = 0.03$ and ρ_K equal 0.03 or 0.003. (c) Fraction of the phosphorylated substrate, ρ_{S_p}/ρ_S , for $c = 10d$, $\rho_P = 0.03$, and ρ_K equal 0.03, 0.01, or 0.003.

role in regulatory pathways. Initial stages of signaling employ numerous types of membrane receptors that transmit signals by means of phosphorylation (and sometimes other modifications) of membrane-bound components. A large share of signal transduction takes place on membranes of various intracellular organelles. Biological membranes are considered crowded environment of relatively low diffusivity (at least an order of magnitude lower than in cytosol), and therefore reactions on membranes are expected to be diffusion-controlled. Importantly, effective diffusion coefficients of various substrates can be modified by transient binding to buffering proteins [35], by the presence of crowding molecules, or through changes of viscoelastic properties of the membrane.

In this study, biochemical reactions on two-dimensional membranes are analyzed by means of Monte Carlo kinetic model on the square-shaped, triangular lattice. For this model, we propose a derivation in which the EMRRCs are expressed as the average time, τ_u (or τ_p), a substrate molecules spends between antagonistic reactions. This time, in turn, is the sum of time to find the antagonistic enzyme molecule, τ_{u_1} (or τ_{p_1}), and time to react after the first encounter with the enzyme molecule, τ_{u_2} (or τ_{p_2}). As the time τ_{u_2} (or τ_{p_2}) was found to be simply $\tau_{u_2} = 1/(c\rho_K)$ (or $\tau_{p_2} = 1/(d\rho_P)$), the main difficulty is in calculating time to find the antagonistic enzyme molecule, τ_{u_1} (or τ_{p_1}).

In solving this problem, we first noticed that phosphorylation and dephosphorylation reactions are correlated in space and time. Intuitively, it is clear when one

enzyme, e.g., kinase, is much more abundant than the other enzyme. Then one may expect that after phosphorylation the search for the phosphatase molecules starts from one of the kinase molecules located in the vicinity of the phosphatase molecule (which had previously dephosphorylated the substrate molecule), rather than from a random place with respect to the locations of phosphatase molecules. As a result, τ_{u_1} (or τ_{p_1}) depends on concentrations of both enzymes. After noticing this fact, we estimated τ_{u_1} and τ_{p_1} using the formula of Montroll [33], which gives the average number of steps before trapping the random walker in a field of traps of concentration ρ . Coefficients of this formula were calculated by Montroll [33] for the case of periodically distributed traps; here, for the case of randomly distributed traps, we assumed that the first, leading-order coefficient has the same value as in the Montroll formula, and fit the value of the second coefficient using the results of numerical simulations.

The resulting macroscopic phosphorylation reaction rate coefficient c_{eff} has an intuitive form: it is half of the harmonic average of the microscopic phosphorylation rate constant, c , and the effective motility, \tilde{M} , divided by a slowly decreasing logarithmic function of enzyme concentration, $\rho_E = \rho_K + \rho_P$:

$$c_{\text{eff}} = \left(\frac{1}{c} + \frac{1}{\tilde{M}} f(\rho_E) \right)^{-1}. \quad (24)$$

In the case when $c \ll \tilde{M}$, i.e., in the reaction-controlled limit, we have $c_{\text{eff}} \approx c$, while in the opposite, diffusion-

controlled limit, $c \gg \tilde{M}$, $c_{\text{eff}} \approx \tilde{M}/f(\rho_E)$. In the last limit the logarithmic dependence of c_{eff} on enzyme concentration, $f(\rho_E) \propto \log(1/\rho_E)$, follows from the fact that the expected number of steps $w(\rho)$ till trapping in a system of randomly distributed traps with density ρ scales as $w(\rho) \propto \rho^{-1} \log(\rho^{-1})$ in the limit of $\rho \rightarrow 0$, when starting from a random position. In our case, the search for a kinase molecule starts after dephosphorylation, which takes place in an approximately random position with respect to the kinases. In the case when search starts from a site neighboring a trap, the expected number of steps scales as $\tilde{w}(\rho) \propto \rho^{-1}$. Therefore, for example, in the classic reversible dimerization problem, an A molecule after the $A \cdot B$ dimer dissociation needs on average $\tilde{w}(\rho_B) = \rho_B^{-1}$ steps to find the same or another B molecule. This constitutes the main difference between reactions involving two antagonistic enzymes and simple reversible reactions.

Equation (24) together with analogous equation for d imply that when microscopic phosphorylation and dephosphorylation rate constants c and d differ, c_{eff} and d_{eff} scale differently with the motility. As a result, the steady-state phosphorylated substrate fraction can depend on the diffusivity. This is in contrast to single-reaction processes such as the reversible dimerization reaction $A + B \rightleftharpoons A \cdot B \xrightleftharpoons[k]{q} C$ (considered in Appendix C) where the steady-state concentration of C does not depend on the diffusion coefficient.

The derived EMRRCs and the steady-state value of the phosphorylated substrate fraction agree with the numerical estimates with reasonable accuracy. Based on analytical considerations and results of numerical simulations, we may conclude that in the range of parameters

$$m \in (0, \infty), \quad \rho_K \in (0, 0.03), \quad \rho_P \in (0, 0.03), \quad \rho_S \in (0, 0.1) \quad (25)$$

the analytical estimates of EMRRCs and the phosphorylated substrate fraction ρ_{S_p}/ρ_S satisfy:

- for $c = d$: [EMRRC relative error] < 5% & $[\rho_{S_p}/\rho_S]$ is exact;
- for $c \neq d$ with $c/d \in (0.01, 100)$: [EMRRC relative error] < 20% & $[\rho_{S_p}/\rho_S \text{ error}] < 0.05$.

Still, one should be aware of limitations of the on-lattice model, discussed in the last subsection of Results. These limitations can render our approximation non-satisfactory for dense systems characterized by a very small diffusivity.

In summary, the proposed analysis is able to capture the behavior of the system in which the steady state is qualitatively controlled by diffusion. For low diffusivity, i.e., when reaction kinetics is diffusion-controlled, the steady state is imposed by the more abundant enzyme, while for high diffusivity, i.e., in the reaction-controlled limit, it is imposed by the enzyme which has higher effective activity. More work and a more detailed description is needed in the case of high concentration of enzymes and membrane crowders that can maintain membrane proteins close to the percolation threshold [36]. In this

limit, various subcellular environments exist on the verge of the sol-gel transition [37], and one can expect the existence of localized, temporal abrupt changes of effective diffusivity which can impact biochemical reaction kinetics implicated in signal transduction [38].

ACKNOWLEDGMENTS

We thank Frank den Hollander from Leiden University for sharing information on trapping times in the system of randomly distributed traps. This study was supported by the Polish National Science Center grants 2013/09/N/NZ2/02631 (decision NCN-KR-0011/253/2/13) and 2014/13/B/NZ2/03840. MK is FNP Start 2015 stipendist. Numerical simulations were carried out using the Zeus supercomputer in Krakow and the Grafen computer cluster of the Ochota Biocenter.

Appendix A: Effective motility

Here, we briefly summarize the influence of molecular crowding on the effective motility, \tilde{m} . As discussed before [3], the effective motility of a molecule having motility m depends on both the concentration of crowding molecules, ρ_C , and their motility, m_C . By the crowding molecules we understand those whose presence in a lattice site prevents the considered molecule from moving to that lattice site. The expression for \tilde{m} reads:

$$\tilde{m} = m f(\rho_C, g) (1 - \rho_C), \quad (\text{A1})$$

where f is the correlation function that can be approximated by the following formula [34, 39]:

$$f(\rho_C, g) = \frac{\{[(1-g)(1-\rho_C)f_0 + \rho_C]^2 + 4g(1-\rho_C)f_0^2\}^{1/2}}{2g(1-\rho_C)f_0} - \frac{[(1-g)(1-\rho_C)f_0 + \rho_C]}{2g(1-\rho_C)f_0}, \quad (\text{A2})$$

where

$$f_0 = (1-a)/[1+a(2g-1)] \quad (\text{A3})$$

and g is the ratio of m/m_C . The coefficient a used in Eq. (A3) depends on the lattice type; for triangular lattice (considered here) $a = 0.282$, for square lattice $a = 1 - 2/\pi$ and for honeycomb (or hexagonal) lattice $a = 1/2$ [40]. Since we consider only the case when all molecules have the same motility ($g = 1$), Eq. (A1) simplifies to

$$\tilde{m}(m, \rho_C, 1) = m \frac{\sqrt{\rho_C^2 + 4(1-\rho_C)\left(\frac{1-a}{1+a}\right)^2} - \rho_C}{2\left(\frac{1-a}{1+a}\right)}. \quad (\text{A4})$$

Recall that in the present model we assume that neither two enzyme molecules nor two substrate molecules

can enter the same lattice site. This means that enzyme as well as substrate molecules play the role of crowding agents only for themselves. Accordingly, \tilde{m}_X for $X \in \{S, K, P\}$ is given by:

$$\tilde{m}_X = \begin{cases} \tilde{m}(m_X, \rho_S, 1) & \text{for } X = S, \\ \tilde{m}(m_X, \rho_K + \rho_P, 1) & \text{for } X \in \{K, P\}. \end{cases} \quad (\text{A5})$$

Appendix B: Estimation of $w(\rho)$

Assuming that a walker has the same probability of starting from any non-trapping site, Montroll [33] obtained an analytical asymptotic formula for the average number of steps of a random walker, for walks on lattices with periodic distributions of traps, of concentration ρ , or, equivalently, on finite lattices of volume $V = 1/\rho$ with periodic boundary conditions containing a single trap. The approximate formula reads:

$$w_P(1/V) = \alpha V \log V + \beta V + \gamma + \mathcal{O}(1/V), \quad (\text{B1})$$

where α is constant for a particular lattice structure ($\alpha = 1/\pi$ for square lattice, $\alpha = \sqrt{3}/(2\pi)$ for triangular lattice), whereas β and γ depend also on the shape of the reactor. For a triangular lattice and a square-shaped reactor their values are $\beta \approx 0.235$ and $\gamma \approx -0.251$. We restricted ourselves to two first terms of the right-hand side of Eq. (B1). As discussed by Montroll [33], the formula in Eq. (B1) agrees almost perfectly (with the error smaller than 0.1% for lattices of $V \geq 16$) with exact values.

To obtain the EMRRCs for large lattices with multiple enzyme molecules we need to estimate $w(\rho) = w(1/V)$ in the case when traps are randomly distributed. Up to our best knowledge, despite several theoretical, e.g. Ref. 41, and numerical attempts, e.g. Refs. 42 and 43, this problem remains unsolved, i.e., precise estimates for $w(\rho)$ are not known [44]. Thus, we estimate $w(\rho)$ in numerical simulations (as described in Methods) and then fit the formula analogous to that obtained by Montroll [33] (cf. Eq. (2.16) in Ref. 41), i.e.,

$$w_R(\rho) = \alpha' \rho^{-1} \log(\rho^{-1}) + \beta' \rho^{-1}, \quad (\text{B2})$$

assuming that $\alpha' = \alpha$. Through fitting we obtained $\beta' = 1.00$. Use of α' and β' which were fitted simultaneously does not decrease the error.

We verified the accuracy of our approach by performing analogous simulations for periodic distribution of traps, i.e., in the case when analytical results are known. The small discrepancy between our numerical estimates and the formula derived by Montroll [33] (Fig. 7) justifies our numerical approach and suggests a reasonable accuracy of the fitted coefficient β' when traps are distributed randomly.

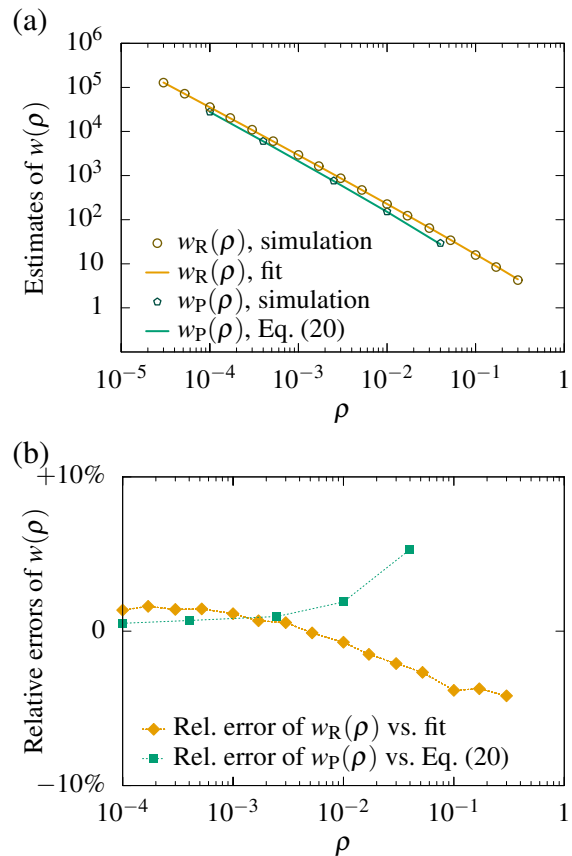


FIG. 7. Average number of steps of a random walker before trapping in periodically and randomly distributed traps. (a) Numerical estimates of $w_R(\rho)$ (random traps) and $w_P(\rho)$ (periodic traps) versus best fit (with $\alpha' = \alpha = \sqrt{3}/(2\pi)$, with fitted $\beta = 1.00$) or the Montroll formula [33] ($\alpha = \sqrt{3}/(2\pi)$ and $\beta = 0.235$). (b) The relative error between numerical estimate and fit, (simulation - fit)/fit, and between numerical estimate and Montroll formula, (simulation - Montroll)/Montroll, see Ref. 33. The fit was obtained for trap concentrations $\rho \in [0.00003; 0.03]$, i.e., when the concentration of traps is low enough so the asymptotic formula can hold but simultaneously the number of traps is not smaller than 30.

Appendix C: Reversible dimerization problem

We consider the classical reversible dimerization reaction $A+B \rightleftharpoons A \cdot B \xrightleftharpoons[k]{q} C$, where $A \cdot B$ denotes the geminate A, B pair that occupies a single lattice site, while C denotes A, B heterodimer. Let ρ_C denote concentration of heterodimers and let ρ_A, ρ_B denote concentrations of A and B molecules that are free or in a geminate pair. This is $\rho_A = \rho_{A_{\text{tot}}} - \rho_C$ and $\rho_B = \rho_{B_{\text{tot}}} - \rho_C$, where $\rho_{A_{\text{tot}}}$ and $\rho_{B_{\text{tot}}}$ are the total concentrations of A and B molecules.

Since the molecules A and B are allowed to enter the same site, their positions are independent. Therefore, the geminate pair concentration will be given by $\rho_{A \cdot B} = \rho_A \rho_B$. In the steady state, geminate pairs $A \cdot B$ are in equilibrium with heterodimers C , i.e., $0 =$

$d\rho_C/dt = k\rho_{A\cdot B} - q\rho_C$, which implies

$$\rho_C = \frac{k}{q} \rho_A \rho_B. \quad (\text{C1})$$

This agrees with the classic formula obtained in the Brownian dynamics model (see, e.g., Ref. 21). The formula implies that steady state concentrations are independent of diffusion, which is in contrast to the more complex reaction scheme studied in this paper. We use this classic formula to check the accuracy of our numerical approach. In Fig. 8 we numerically calculate $q\rho_C/(k\rho_A\rho_B)$ as a function of motility, showing that the error introduced by our numerical scheme is comparable to the statistical error of order of 1% for scaled motilities: $m/k \in (0.01, 100)$.

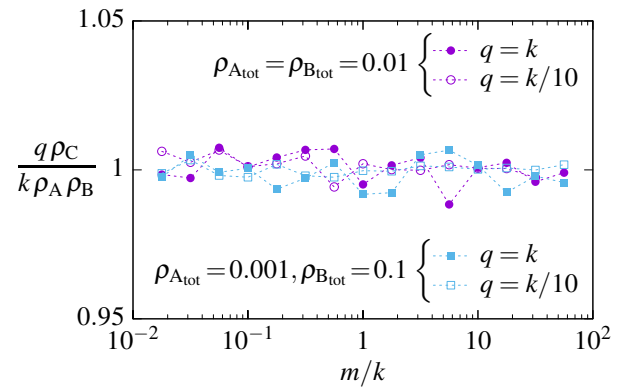


FIG. 8. Reversible dimerization problem: comparison of the numerically calculated steady-state concentrations with the analytical expression, Eq. (C1). Value of the expression $q\rho_C/(k\rho_A\rho_B)$ is plotted as a function of scaled motility, m/k . Four combinations of parameters $\rho_{A_{\text{tot}}}$, $\rho_{B_{\text{tot}}}$, k and q are considered.

-
- [1] O. Dushek, J. Goyette, and P. A. van der Merwe, “Non-catalytic tyrosine-phosphorylated receptors.” *Immunol Rev* **250**, 258–276 (2012).
- [2] H.-X. Zhou, G. Rivas, and A. P. Minton, “Macromolecular crowding and confinement: biochemical, biophysical, and potential physiological consequences.” *Annu Rev Biophys* **37**, 375–397 (2008).
- [3] P. Szymańska, M. Kochańczyk, J. Miękiś, and T. Lipniacki, “Effective reaction rates in diffusion-limited phosphorylation-dephosphorylation cycles,” *Phys. Rev. E* **91**, 022702 (2015).
- [4] M. von Smoluchowski, “Versuch eine mathematischen Theorie der Koagulationskinetik kolloidaler lösungen.” *Z. phys. Chem.* **92**, 129–168 (1917).
- [5] F. C. Collins and G. E. Kimball, “Diffusion-controlled reaction rates,” *J. Colloid Sci.* **4**, 425–437 (1949).
- [6] K. R. Naqvi, “Diffusion-controlled reactions in two-dimensional fluids: Discussion of measurements of lateral diffusion of lipids in biological membranes,” *Chem. Phys. Lett.* **28**, 280–284 (1974).
- [7] C. A. Emeis and P. L. Fehder, “Microscopic mechanism for diffusion and the rates of diffusion-controlled reactions in simple liquid solvents,” *J. Am. Chem. Soc.* **92**, 2246–2252 (1970).
- [8] D. C. Torney and H. M. McConnell, “Diffusion-limited reaction rate theory for two-dimensional systems,” *Proc. R. Soc. Lond. A Mat.* **387**, 147–170 (1983).
- [9] D. Toussaint and F. Wilczek, “Particle–antiparticle annihilation in diffusive motion,” *J. Chem. Phys.* **78**, 2642–2647 (1983).
- [10] C. E. Allen and E. G. Seebauer, “Surface diffusivities and reaction rate constants: Making a quantitative experimental connection,” *J. Chem. Phys.* **104**, 2557–2565 (1996).
- [11] A. Szabo, “Theory of diffusion-influenced fluorescence quenching,” *J. Phys. Chem.* **93**, 6929–6939 (1989).
- [12] H.-X. Zhou, “Theory and simulation of the influence of diffusion in enzyme-catalyzed reactions,” *J. Phys. Chem. B* **101**, 6642–6651 (1997).
- [13] H. Kim, M. Yang, M.-U. Choi, and K. J. Shin, “Diffusion influence on Michaelis–Menten kinetics,” *J. Chem. Phys.* **115**, 1455–1459 (2001).
- [14] S. Park and N. Agmon, “Theory and simulation of diffusion-controlled Michaelis–Menten kinetics for a static enzyme in solution,” *J. Phys. Chem. B* **112**, 5977–5987 (2008).
- [15] S. Park and N. Agmon, “Concentration profiles near an activated enzyme,” *J. Phys. Chem. B* **112**, 12104–12114 (2008).
- [16] Ya. B. Zel’dovich and A. A. Ovchinnikov, “Asymptotic form of the approach to equilibrium and concentration fluctuation,” *JETP Lett.* **26**, 440–442 (1977).
- [17] O. G. Berg, “On diffusion-controlled dissociation,” *J. Chem. Phys.* **31**, 47–57 (1978).
- [18] N. Agmon and A. Szabo, “Theory of reversible diffusion-influenced reactions,” *J. Chem. Phys.* **92**, 5270–5284 (1990).
- [19] A. Szabo, “Theoretical approaches to reversible diffusion-influenced reactions: Monomer–excimer kinetics,” *J. Chem. Phys.* **95**, 2481–2490 (1991).
- [20] A. L. Edelstein and N. Agmon, “Equilibration in reversible bimolecular reactions,” *J. Phys. Chem.* **99**, 5389–5401 (1995).
- [21] I. V. Gopich and A. Szabo, “Kinetics of reversible diffusion influenced reactions: The self-consistent relaxation time approximation,” *J. Chem. Phys.* **117**, 507 (2002).
- [22] K. Takahashi, S. Tănase-Nicola, and P. R. ten Wolde, “Spatio-temporal correlations can drastically change the response of a MAPK pathway,” *Proc. Natl Acad. Sci. USA* **107**, 2473–2478 (2010).
- [23] O. Dushek, P. A. van der Merwe, and V. Shahrezaei, “Ultrasensitivity in multisite phosphorylation of membrane-anchored proteins.” *Biophys. J.* **100**, 1189–1197 (2011).

- [24] J. S. van Zon, M. J. Morelli, S. Tănase-Nicola, and P. R. ten Wolde, “Diffusion of transcription factors can drastically enhance the noise in gene expression,” *Biophys. J.* **91**, 4350–4367 (2006).
- [25] Ch. C. Govern, M. K. Paczosa, Chakraborty A. K., and E. S. Huseby, “Fast on-rates allow short dwell time ligands to activate T cells,” *Proc. Natl Acad. Sci. USA* **107**, 8724–8729 (2010).
- [26] A. V. Popov and N. Agmon, “Exact solution for the geminate $abcd$ reaction,” *J. Chem. Phys.* **117**, 5770 (2002).
- [27] S. Park, K. J. Shin, and N. Agmon, “Exact solution of the excited-state geminate $A^* + B \leftrightarrow C^* + D$ reaction with two different lifetimes and quenching,” *J. Chem. Phys.* **121**, 868–876 (2004).
- [28] S. Park, K. J. Shin, A. V. Popov, and N. Agmon, “Diffusion-influenced excited-state reversible transfer reactions, $A^*+B=C^*+D$, with two different lifetimes: Theories and simulations,” *J. Chem. Phys.* **123**, 034507 (2005).
- [29] A. Szabo and H.-X. Zhou, “Role of diffusion in the kinetics of reversible enzyme-catalyzed reactions,” *Bull. Kor. Chem. Soc.* **33**, 925 (2012).
- [30] P. J. Zuk, M. Kočańczyk, J. Jaruśzewicz, W. Bednorz, and T. Lipniacki, “Dynamics of a stochastic spatially extended system predicted by comparing deterministic and stochastic attractors of the corresponding birth-death process.” *Phys. Biol.* **9**, 055002 (2012).
- [31] M. Kočańczyk, J. Jaruśzewicz, and T. Lipniacki, “Stochastic transitions in a bistable reaction system on the membrane.” *J. R. Soc. Interface* **10**, 20130151 (2013).
- [32] D. T. Gillespie, “Exact stochastic simulation of coupled chemical reactions,” *J. Phys. Chem.* **81**, 2340–2361 (1977).
- [33] E. W. Montroll, “Random walks on lattices. III. Calculation of first-passage times with application to exciton trapping on photosynthetic units,” *J. Math. Phys.* **10**, 753–765 (1969).
- [34] H. van Beijeren and R. Kutner, “Mean square displacement of a tracer particle in a hard-core lattice gas,” *Phys. Rev. Lett.* **55**, 238 (1985).
- [35] B. Kaźmierczak and Z. Peradzyński, “Calcium waves with fast buffers and mechanical effects.” *J. Math. Biol.* **62**, 1–38 (2011).
- [36] B. J. Sung and A. Yethiraj, “Lateral diffusion of proteins in the plasma membrane: spatial tessellation and percolation theory.” *J. Phys. Chem. B* **112**, 143–149 (2008).
- [37] P. Li, S. Banjade, H.-Ch. Cheng, S. Kim, B. Chen, L. Guo, M. Llaguno, J. V. Hollingsworth, D. S. King, S. F. Banani, P.S. Russo, Q.-X. Jiang, B. T. Nixon, and M. K. Rosen, “Phase transitions in the assembly of multivalent signalling proteins.” *Nature* **483**, 336–340 (2012).
- [38] K. Jaqaman, H. Kuwata, N. Touret, R. Collins, W. S. Trimble, G. Danuser, and S. Grinstein, “Cytoskeletal control of CD36 diffusion promotes its receptor and signaling function.” *Cell* **146**, 593–606 (2011).
- [39] P. F. F. Almeida and W. L. C. Vaz, “Lateral diffusion in membranes,” *Handbook of Biological Physics* **1**, 305–357 (1995).
- [40] K. Compaan and Y. Haven, “Correlation factors for diffusion in solids,” *Trans. Faraday Soc.* **52**, 786–801 (1956).
- [41] W. Th. F. Den Hollander, “Random walks on lattices with randomly distributed traps. I. The average number of steps until trapping,” *J. Stat. Phys.* **37**, 331–367 (1984).
- [42] P. Scheunders and J. Naudts, “Random walks on lattices with a random distribution of perfect traps,” *Z. Phys. B* **73**, 551–553 (1989).
- [43] G. T. Barkema, P. Biswas, and H. van Beijeren, “Diffusion with random distribution of static traps,” *Phys. Rev. Lett.* **87**, 170601 (2001).
- [44] After the acceptance of the manuscript, we learned from Frank den Hollander that based on results from Refs. 41 and 45, in the case of randomly distributed traps the following approximate analytical formula for the average number of steps before trapping can be obtained:

$$w_R^*(\rho) = \frac{A}{\rho} \left(\log \frac{C}{\rho} + \log \log \frac{C}{\rho} + \log \log \frac{C}{\rho} / \log \frac{C}{\rho} + 2K / \log \frac{C}{\rho} + \dots \right),$$
where $A = \sqrt{3}/(2\pi)$, $C = 8\sqrt{3}\pi$, $K \simeq 1.171953$. This formula is thought to be exact in the limit of $\rho \rightarrow 0$ and does not require parameter fitting, which is an undisputed advantage. In the regime explored in this paper, however, its accuracy is not better than that of formula (B2) and it produces more complex expressions for c_{eff} and d_{eff} .
- [45] F. S. Henyey and V. Seshadri, “On the number of distinct sites visited in 2D lattices,” *J. Chem. Phys.* **76**, 5530 (1982).